

WHAT IS THE ACCRETION RATE IN NGC 4258?

CHARLES F. GAMMIE¹ AND RAMESH NARAYANHarvard-Smithsonian Center for Astrophysics, MS-51
60 Garden St., Cambridge, MA 02138

AND

ROGER BLANDFORD

Theoretical Astrophysics, Caltech 130-33, Pasadena, CA 91125

Draft version October 1, 2018

ABSTRACT

We consider the implications of recent infrared and radio observations of the nucleus of NGC 4258. There is no direct evidence that the nucleus has been steadily accreting on the viscous timescale of the outer masing disk, which is $\gtrsim 10^9$ yr. Thus the mass accretion rate in the outer disk need not be the same as in the inner accretion flow where most of the gravitational binding energy is released. We show that an advection-dominated flow model with a transition radius of $\sim (10 - 100)GM/c^2$ (where M is the mass of the hole) and $\dot{M} \approx 10^{-2} M_\odot \text{yr}^{-1}$ is consistent with the observed spectrum from radio to X-rays. We also show that a thin (flat or warped) disk can fit the observed fluxes outside the X-ray band. The X-rays can be explained by means of a corona in such a model, but the absence of radio emission from the location of the putative central black hole provides a serious constraint on the properties of the corona. A wide range of accretion rates, $10^{-4} \lesssim \dot{M} \lesssim 10^{-2} M_\odot \text{yr}^{-1}$, can be made to fit the data, but the most “natural” models have $10^{-3} \lesssim \dot{M} \lesssim 10^{-2} M_\odot \text{yr}^{-1}$. Physical conditions in the observed VLBI jet features can also be related to conditions in the inner accretion flow. We conclude with a list of future observations that might help to constrain the accretion rate.

Subject headings: accretion, accretion disks — black hole physics — radio jets

1. INTRODUCTION

Most measurements of the physical properties of astronomical objects are fortunate to obtain an accuracy of a factor of two. The rare instances when more precise measurements are possible offer significant opportunities for advancing our knowledge, and so it is worth investing some effort to understand these objects in detail. The orbiting water maser spots in NGC 4258 provide one of these rare instances.

Water maser emission was first detected in the nucleus of NGC 4258 by Claussen et al. (1984). It was soon realized that the masers might lie in a disk (Claussen & Lo (1986)). Nakai et al. (1993) discovered high velocity maser emission, which Watson & Wallin (1994) quickly interpreted as a natural outcome of maser emission from a disk. VLBI observations (Greenhill et al. (1995b), Miyoshi et al. (1995), Moran et al. (1995), Herrnstein, Greenhill, & Moran (1996)) demonstrated that the maser spots are positioned on the sky as one would expect for a nearly edge-on thin disk. A model fit to

the maser spots allows one to determine the central mass (Herrnstein (1997)). By measuring maser spot accelerations (Haschick & Baan (1990), Haschick et al. (1994), Greenhill et al. (1995c), Greenhill et al. (1995a), Herrnstein (1997)), or proper motions (Herrnstein (1997)) one can also directly determine a geometric distance.

The measurement of an accurate mass and distance eliminate two of the principal uncertainties that plague efforts to understand the physics of active galactic nuclei (AGN). The mass of the central object in NGC 4258 (which we will freely refer to as a black hole) is $(4 \pm 0.25) \times 10^7 M_\odot$ (Herrnstein (1997); 1σ). The distance is measured to be 7.3 ± 0.3 Mpc, with independent and consistent results from measurements of maser spot acceleration and maser spot proper motion (Herrnstein et al. (1997c)).

One of the other main uncertainties that plagues AGN studies is the accretion rate \dot{M} . The accretion rate in NGC 4258 has been controversial, and there are a number of estimates in the literature: Neufeld & Maloney (1995) (hereafter NM), $7 \times 10^{-6} \alpha_{-1} M_\odot \text{yr}^{-1}$,

¹Also Isaac Newton Institute, 20 Clarkson Rd., Cambridge CB3 0EH, UK

where $\alpha = 0.1\alpha_{-1} \lesssim 1$ is the usual dimensionless angular momentum diffusion coefficient of accretion disk theory (Shakura & Sunyaev (1973), Pringle (1981)); Lasota et al. (1996), $0.014\alpha_{-1} M_{\odot} \text{ yr}^{-1}$; Cao & Jiang (1997), $8 \times 10^{-5}\alpha_{-1} M_{\odot} \text{ yr}^{-1}$; Maoz & McKee (1997), $7 \times 10^{-3} M_{\odot} \text{ yr}^{-1}$; Kumar (1997), $1.5 \times 10^{-3} M_{\odot} \text{ yr}^{-1}$. These estimates differ because of disagreements about the nature and efficiency of angular momentum transport in disks and, to a lesser degree, because of disagreements about the heating and cooling physics in various parts of the accretion flow. The purpose of this paper is to clarify some of these differences, propose observational tests that reduce the number of acceptable models, and thereby narrow the range of uncertainty in \dot{M} .

We begin in §2 by asking what the masing disk might tell us about the accretion rate. In §3 we give a critical review of the pertinent data; in §4 we consider models for the inner accretion flow; in §5 we consider implications of observations of the jet. A discussion and summary of interesting observational and theoretical problems follows in §6.

2. MASING DISK

Most estimates of the accretion rate in NGC 4258 are based on observations of the masing disk and the assumption that the disk is in a steady state ($d\dot{M}(r)/dr = 0$) from the masing disk in to the black hole, where most of the gravitational binding energy is released (NM, Cao & Jiang (1997), Maoz & McKee (1997), Kumar (1997)). But is the masing disk in a steady state? In the absence of significant external torques (e.g. a magnetohydrodynamic wind) one expects a steady state to be achieved on the viscous timescale $t_v \equiv (\alpha\Omega)^{-1} \times (r/H)^2$, if mass is steadily supplied to the disk from $r \gtrsim 0.26 \text{ pc}$.

In the masing disk, $t_v = 2.6 \times 10^9 \alpha_{-1}^{-1} (200 \text{ K}/T)(r/0.2 \text{ pc})^{1/2} \text{ yr}$.² This is a significant fraction of a Hubble time. We know of no direct evidence that mass has been steadily supplied to the nucleus of NGC 4258, or to any active nucleus, on this timescale. Thus there is no direct support for the assumption that the disk is in a steady state.

NGC 4258 contains an unusual, kpc-scale jet detected in optical lines (Courtès & Cruvellier (1961)), radio continuum (van der Kruit et al. (1972)), and X-rays (Cecil et al. (1995a)). If the jet is produced in the immediate vicinity of the black hole, and the jet mass loss rate is closely coupled to the accretion rate, as is commonly believed, then it provides a fossil record of past accretion. The characteristic timescale for the jet is $t_J = R/V_J = 2.4 \times 10^6 (R/5 \text{ kpc})(2000 \text{ km sec}^{-1}/V_J) \text{ yr}$ where V_J is

²An optically thin coronal component with $T \sim 8000 \text{ K}$, as suggested by NM, might carry a large \dot{M} with a small viscous timescale. But in the NM model, at least, most of the mass flux is carried in the cool, optically thick component at the inner edge of the masing disk.

the jet radial velocity. More detailed models of the jet suggest an age of at least 10^6 to 10^7 yr (e.g. van Albada & van der Hulst (1982), Martin et al. (1989)). Thus the jet provides a record over only a small fraction of the masing disk viscous timescale. The jet is roughly continuous over its length, however (there are no lengthy gaps in the jets: see for example Figure 2 of Cecil et al. (1995a)), which suggests approximately steady accretion over a time t_J . For standard α disk models for the inner accretion flow we find $t_v = t_J \sim 10^6 \text{ yr}$ at $r \sim 10^3 GM/c^2$ (the precise value depends on the accretion rate, α , etc.). Thus only a small region of the accretion flow in NGC 4258 needs to be in a steady state.

3. CRITICAL REVIEW OF DATA

3.1. Nuclear Spectral Energy Distribution

Chary & Becklin (1997) have recently reported J,H, and K band (1.25, 1.65, 2.21 μm) observations of NGC 4258 in 0.6" seeing. Using the J band image as a baseline, they subtract a scaled J band image from the H and K images and find a nuclear emission excess consistent with a point source. The excess is 1.1 mJy at H and 4.5 mJy at K. It is then possible to deduce the extinction and intrinsic luminosity of the source if the extinction follows a standard form deduced from the local interstellar medium (Cardelli et al. (1989)) and if the intrinsic spectrum has an approximately power-law form over the region of interest ($f_{\nu} \sim \nu^s$):

$$A_V = 20.1(1 + 0.21s) \text{ mag}, \quad (1)$$

$$\log(\nu L_{\nu}(H)/\text{erg s}^{-1}) = 41.63 + 0.32s, \quad (2)$$

$$\log(\nu L_{\nu}(K)/\text{erg s}^{-1}) = 41.51 + 0.19s. \quad (3)$$

The spectral index s might reasonably range from $\sim 1/3$ for the classical thin disk spectrum to ~ -1 , which is a typical optical spectral index for an unobscured AGN. The implied flux at J is $0.2(2.62)^s \text{ mJy}$, which is small, justifying the use of the J band image as a baseline. Taking $R_V = 3.1$ (Spitzer (1978)), the extinction implies an obscuring column

$$N_H = 3.8 \times 10^{22} (1 + 0.21s)(Z_{\odot}/Z) \text{ cm}^{-2} \quad (4)$$

($Z \equiv$ metallicity) or, assuming cosmic abundance of helium,

$$\Sigma = 0.09(1 + 0.21s)(Z_{\odot}/Z) \text{ g cm}^{-2}. \quad (5)$$

These estimates are sensitive to the assumed extinction curve, since

$$\frac{d \ln \nu L_{\nu}(H)}{d \ln (A_H/A_K)} = -5.3 - 1.1s, \quad (6)$$

and

$$\frac{dA_V}{d\ln(A_H/A_K)} = -50 - 10s. \quad (7)$$

Evidently 10% variations in extinction can lead to factor-of-two errors in the intrinsic luminosity.

Makishima et al. (1994) have reported X-ray observations of NGC 4258 with ASCA. They fit a four component model to the spectrum, including an obscured power law, an iron line, a Raymond-Smith plasma, and thermal bremsstrahlung. They find an integrated luminosity for the power law component in the 2 to 10 keV band of $(4.4 \pm 1.1) \times 10^{40} \text{ erg s}^{-1}$ (at 7.3 Mpc), and an absorbing column $N_H = (1.5 \pm 0.2) \times 10^{23} \text{ cm}^{-2} Z_\odot/Z$. Assuming a cosmic abundance of helium, this implies $\Sigma = 0.36 \text{ g cm}^{-2} (Z_\odot/Z)$. The X-ray column is a factor of 4 larger than the column inferred from infrared extinction which, given the uncertainties, may be considered reasonably good agreement. Indeed, the two columns need not agree if the IR emitting material is also producing the X-ray absorption. The integrated luminosity implies $\nu L_\nu = 2.7 \times 10^{40} \text{ erg s}^{-1}$ at 4.5 keV, taking the mean of νL_ν across the 2 to 10 keV band.

Makishima et al.'s data are now publicly available through the ASCA data archives. We have tried fitting only an absorbed power law to the 2.5 to 10 keV data. While the total luminosity is robust, being mostly determined by the flux near 10 keV, our absorption column is lower than the Makishima et al. value. This suggests that the derived absorption column is sensitive to the presence of the thermal bremsstrahlung component in the Makishima et al. model, and may be somewhat less reliable than the total luminosity.

Herrnstein et al. (1998) report a 3σ upper limit on the 22 GHz flux from the neighborhood of the compact object of 0.22 mJy, or $\nu L_\nu = 3.1 \times 10^{35} \text{ erg s}^{-1}$.

Rieke & Lebosky (1978) report a detection in a $5''$ aperture at $10\mu\text{m}$ of 100 mJy, or $\nu L_\nu = 1.9 \times 10^{41} \text{ erg s}^{-1}$. A consistent result at similar aperture size is reported by Cizdziel et al. (1985). Because of the large aperture these are upper limits.

Finally, the nucleus has been detected in polarized optical light by Wilkes et al. (1995). The polarized continuum has $f_\nu \sim \nu^{-1.1 \pm 0.2}$, with an amplitude $\nu L_\nu = 1.1 \times 10^{39} \text{ erg s}^{-1}$. The polarized spectral lines have FWHM of order 2500 km sec^{-1} , a velocity characteristic of radii just within the radius of the masing disk. These results offer only weak constraints on \dot{M} because the composition and distribution of the scattering medium are poorly constrained. Following Wilkes et al. we will regard the polarized emission as providing an upper limit on νL_ν of $4 \times 10^{43} \text{ erg s}^{-1}$.

3.2. Jet

The jet in NGC 4258 is observed at milliarcsecond scales in 22 GHz continuum with the VLBA (Herrnstein et al. (1997a)) and at arcsecond and larger scales in the radio, optical, and X-ray.

The VLBA jet was discovered by Herrnstein et al. (1997a), while higher signal-to-noise data has recently been presented by Herrnstein et al. (1998). The northern jet has flux density $\simeq 3 \text{ mJy}$, is variable on a timescale of weeks, and is unresolved. Its mean location is about 0.014 pc ($= 17 \text{ light-days} = 7500 GM/c^2$) north of the best-fit location for the compact object, and its position varies significantly with time. The southern jet has flux density $\simeq 0.5 \text{ mJy}$, has not varied significantly in flux or position, and is also unresolved. It is located about 0.035 pc ($= 43 \text{ light-days} = 19,000 GM/c^2$) south of the best-fit location for the compact object. The difference in brightness between northern and southern jet is attributed by Herrnstein et al. (1997a) to free-free absorption in the masing disk. The emitting blobs are approximately due south and north of the compact central object (Herrnstein et al. (1998)). This is consistent with the jet being normal to the outer, masing disk and suggests that the disk is not strongly warped, at least in position angle, between the masing disk and the radius where the jet is launched.

Radio and X-ray observations show a curious, twisted jet outflow both to the north and the south extending out to $\sim 5 \text{ kpc}$ (summarized in Cecil et al. (1992), Cecil et al. (1995a), Cecil et al. (1995b)). The jet X-ray emission has a power $\sim 2 \times 10^{40} \text{ erg s}^{-1}$ and can be satisfactorily fit by a thermal spectrum with temperature $T_X \sim 3 \times 10^6 \text{ K}$. Associated with this jet are forbidden emission lines which appear to come from locally photoionized shocked plasma. The line widths suggest velocities $\sim 500 \text{ km s}^{-1}$.

4. INNER DISK MODELS

An observed flux F_{obs} suggests a minimum accretion rate $\dot{M}_{min} = 4\pi d^2 F_{obs}/(\epsilon c^2)$, where $\epsilon = 0.1\epsilon_{-1}$ is the accretion efficiency. This is not a rigorous limit since the flow can emit anisotropically and a spinning black hole can provide an additional reservoir of energy. Setting aside these concerns for the moment, it is reasonable to take $\epsilon_{-1} \sim 1$ (recall that the specific binding energy on the last stable circular orbit varies from $0.038c^2$ for retrograde orbits around a maximally rotating black hole to $0.42c^2$ for prograde orbits around a maximally rotating hole; this binding energy is approximately related to the efficiency ϵ of a thin disk accretion flow). Taking the observed flux densities in the infrared, integrating over the band, and adding this to the 2 – 10 keV flux (while this is corrected for absorption, the to-

tal flux is not sensitive to the absorption), we find $\dot{M}_{min} = 10^{-5}\epsilon_{-1}^{-1} M_{\odot} \text{ yr}^{-1}$. This assumes the rest of the spectrum is black (which is not correct given the detection of scattered light in the optical by Wilkes et al. (1995)) and the infrared extinction is zero. A less radically skeptical approach is to set the luminosity equal to the extinction-corrected infrared νL_{ν} . Then $\dot{M}_{min} = 7 \times 10^{-5} (2.1)^s \epsilon_{-1}^{-1} M_{\odot} \text{ yr}^{-1}$.

The rest of the spectrum is not black. By analogy with other AGN, NGC 4258 should have a rather flat spectrum in νL_{ν} . One can then ask what is the minimum luminosity in a power law spectral energy distribution that extends from the optical to 100 keV and passes through the X-ray data point; we find the minimal power law slope is $\nu L_{\nu} \sim \nu^{0.27}$, and the corresponding luminosity is $2.3 \times 10^{41} \text{ erg s}^{-1}$. Adding this to the minimal accretion rate from the infrared point gives $\dot{M}_{min} = (7(2.1)^s + 4) \times 10^{-5} \epsilon_{-1}^{-1} M_{\odot} \text{ yr}^{-1}$, although some of the optical, UV, and soft X-ray flux may be absorbed by a disk and reradiated in the infrared.

So far we have assumed that the accretion flow radiates isotropically, but a thin disk, for example, has $f_{\nu} \sim \cos(i)$, if we ignore the effects of limb-brightening. Since the masing disk inclination is 82° , and the most natural assumption is that the inner disk has the same inclination (although there is no direct evidence for this), there will also be a large additional upward correction in the mass accretion rate, since $\cos(82^{\circ}) \simeq 0.14$. A specific model is required for a quantitative estimate of the inclination correction.

4.1. Thin Disk Model

Suppose that the central engine is just a thin, flat disk that radiates locally like a black body. On the $\nu^{1/3}$ portion of the classical thin disk spectrum,

$$f_{\nu} = 17.8 \dot{M}_{-4}^{2/3} \cos(i) \lambda^{-1/3} \text{ mJy}, \quad (8)$$

where λ is in microns and \dot{M}_{-4} is the accretion rate in units of $10^{-4} M_{\odot} \text{ yr}^{-1}$. Inverting this equation, the required mass accretion rate is

$$\dot{M} \simeq 1.3 \times 10^{-6} f_{\nu}^{3/2} \lambda^{1/2} \cos(i)^{-3/2} M_{\odot} \text{ yr}^{-1}, \quad (9)$$

where f_{ν} is in mJy. Assuming $f_{\nu} \sim \nu^{1/3}$ and $i = 82^{\circ}$, the infrared data of Chary & Becklin require $\dot{M} = 0.011 M_{\odot} \text{ yr}^{-1}$. Notice that the inclination correction is quite large because \dot{M} depends nonlinearly on $\cos(i)$. This also assumes the disk extends down to $r = 0$; if the disk is truncated properly (say at $r = 6GM/c^2$) then \dot{M} must be evaluated numerically: $\dot{M} = 0.013 M_{\odot} \text{ yr}^{-1}$. Thin disk spectra for $i = 0^{\circ}, 45^{\circ}$, and 82° are shown in Figure 1.

There are several effects that might tend to change the accretion rate. First, the inner disk might be inclined differently from the masing disk. If $i = 45^{\circ}$, then the accretion rate can be pushed as low as $0.0012 M_{\odot} \text{ yr}^{-1}$; the order of magnitude change in \dot{M} again follows from the nonlinear dependence of \dot{M} on $\cos(i)$ in eq.(8). It is also possible, however, that the inclination of the inner disk is larger than 82° . Second, the obscuring dust grains might well have a different size distribution than in the local interstellar medium. The sense of the effect of grain size evolution, however, at least in the grain models of Laor & Draine (1993), is to decrease A_H/A_K and so increase the required mass accretion rate.

Third, some of the near-infrared emission may be reprocessed light from the central engine, either in a disk or in a wind (e.g. Königl & Kartje (1994)). Crudely speaking, the light must be reprocessed at $r \sim r_{1500} \sim 2.8 \times 10^3 L_{42}^{1/2} GM/c^2$ corresponding to a characteristic temperature of $1500K$ for near IR emission (dust grains much smaller than $1\mu\text{m}$ can produce H and K band emission from a somewhat larger radius because they radiate inefficiently in the infrared). When is reprocessing important in a disk? Suppose $\mu(r, \phi)$ is the ‘‘obliquity’’ of the disk, which is to say, the angle between the normal to the disk surface and the radius vector, f is the fraction of intercepted radiation that is thermalized in the disk (so $1 - f$ is an effective albedo). Then reprocessing is dominant if $r \gtrsim (GM/c^2)(\epsilon f \cos \mu)^{-1}$. For a thin, flared disk $\cos \mu \sim H/R$. One can then show that, in a standard α disk model over a large range of \dot{M} , reprocessing is not dominant at $r \sim r_{1500}$.

If the disk is warped then $\cos \mu$ can be larger and reprocessing can dominate internal heating. It is not possible to survey the warp parameter space, since a warp is described by two free functions: the inclination $i(r)$ and position angle $p(r)$. A broad range of behavior is possible. For example, the warp could be made sufficiently large so as to cover the central engine (raising the inferred accretion rate); it could also be arranged so that the inner disk is nearly face on (lowering the inferred accretion rate).

As an illustration, however, we have constructed a ‘‘naive’’ warped disk model with only an inclination warp ($p(r) = \text{const.}$) in which the reprocessed light is reradiated as a black body. The disk extends from $r = 6GM/c^2$ to 0.26 pc , as does the flat disk model, and has constant \dot{M} . The effective temperature T_e of the disk is given by $T_e^4 = T_{int}^4 + f_{obl} T_{ext}^4$, where T_{int} is the effective temperature in the absence of external heating, and

$$\sigma T_{ext}^4 = \frac{\epsilon \dot{M} c^2}{4\pi r^2} \quad (10)$$

and $\epsilon = 0.1$. Here f_{obl} is the obliquity factor. If the disk is illuminated on the side facing us, then $f_{obl} \simeq \sin(\phi)|di/d\ln r|$, where ϕ is the disk orbital phase. If the disk is illuminated on the side facing away from us, as it is for half its orbit, then the reprocessing only adds a flux $\sigma T_{ext}^4/\tau$ to our side of the disk, and so, assuming that $\tau \gg (T_{ext}/T_{int})^4$, we set $f_{obl} = 0$.

Figure 2 shows the resulting thin, warped disk spectrum. The warp extends from $r = 100GM/c^2$ to $r = 0.26$ pc with $di/d\ln r = 0.05$. The accretion rate is $8 \times 10^{-4} M_{\odot} \text{ yr}^{-1}$. Three effects combine here to reduce the required accretion rate: (1) reprocessing enhances the $2\mu\text{m}$ flux; (2) reprocessing make the spectrum shallower at $2\mu\text{m}$ thus reducing the reddening correction; (3) the inclination warp changes the inclination of the inner disk from 82° to 61° , thus making the reprocessing portion of the disk more face-on.

Our warped disk model is naive in the sense that the reprocessed emission does not emerge as a blackbody. In particular, dust grains in the disk atmosphere can cause half of the flux intercepted by the disk to reemerge as a dilute blackbody with $T > T_e$. This effect has been considered in the context of quasar disks by Sanders et al. (1989) and Phinney (1989); the same effect has been considered in the context of circumstellar disks by Chiang & Goldreich (1997). In Phinney's quasar models the resulting spectrum has a notch at $\sim 1\mu\text{m}$ related to the onset of dust sublimation at $T \approx 1800$ K. Since the spectrum might then be declining at H and K bands, this could reduce the reddening correction and thus also reduce the required accretion rate.

Reprocessing is ultimately limited, however, by the luminosity of the central accretion flow. Figure 1 also shows a thin disk spectrum for a face-on disk truncated at $r = 6GM/c^2$, with $\dot{M} = 7 \times 10^{-6} M_{\odot} \text{ yr}^{-1}$, corresponding to the model of Neufeld & Maloney (1995) with $\alpha = 0.1$. It would be difficult to produce the observed infrared flux from such a low accretion rate disk even with a highly optimized arrangement of reprocessing material.

A reprocessing model for the H and K band flux can be tested via long term monitoring. If the light is reprocessed, then IR variability should be highly correlated with X-ray variability, with delays on order the light travel time $r_{1500}/c \simeq 5.5 \times 10^5 L_{42}^{1/2}$ s.

Finally, while we have not explicitly fit the X-ray emission using a thin disk plus corona model (e.g. Haardt & Maraschi (1991)), it is generally acknowledged that it is possible to do so, since there are a number of free parameters associated with the corona.

An alternative to the thin disk plus corona model for the inner accretion flow is the two-temperature advection-dominated accretion flow model (ADAF; Ichimaru (1977), Narayan & Yi (1994), Narayan & Yi (1995b), Abramowicz (1995); see Narayan (1997), Narayan et al. (1998) for reviews). ADAFs are optically thin and geometrically thick, with $H/R \sim 1$. They have been used to successfully fit the spectral energy distribution of accretion flows onto both stellar mass and supermassive black holes. In their simplest form, ADAFs approximate the flow as non-radiative, with nested spherical surfaces moving radially inwards with an angular velocity given by the value on the equatorial plane. Radial pressure gradients combine with centrifugal force to oppose gravity and radial motion is fast, though subsonic until it approaches the event horizon. There is hypothesized to be a large viscous stress ($\sim \alpha P$, where P is the pressure) that transports angular momentum radially outward.

The ADAF approach has some dynamical shortcomings. Firstly, it does not take account of angular velocity gradients on spherical surfaces. This appears to be a reasonable approximation far from the black hole in the self-similar region of the flow (cf. Narayan & Yi (1995a)), but the approximation may break down close to the hole, especially close to the symmetry axis. This is relevant for understanding whether the flow forms a funnel and a jet. The indications are that there is no funnel when $\alpha \gtrsim 0.01$ (Narayan, Kato & Honma (1997), Gammie & Popham (1998), Popham & Gammie (1998), though this conclusion is not certain). Secondly, the solutions assume vertical hydrostatic equilibrium, which is suspect in the supersonic region close to the hole. This approximation should not have direct impact on the emergent radiation, though. Finally, in these solutions, the gas has positive Bernoulli constant and always has enough energy to escape the hole (see Narayan & Yi (1994), Narayan & Yi (1995a), Narayan, Kato & Honma (1997)). This arises because of the inevitable, outward radial transport of energy by the viscous stress, which is balanced exactly by inward advective transport of energy. This balance must be maintained everywhere. If it is not, then it is possible that energy may be carried away by a wind (see Blandford (1998), and in preparation).

Counterbalancing these shortcomings is the fact that the ADAF is the only model of hot accretion flows that attempts to calculate the dynamics, thermal structure and radiative spectrum of the gas self-consistently. Other approaches, e.g. coronal models, leave most details of the dynamics unspecified and allow far greater freedom in choosing the properties of the radiating plasma.

4.2. Advection-Dominated Flow Model

Lasota et al. (1996) proposed a model for NGC 4258 which comprises a thin disk extending outward from the transition radius r_{tr} and an ADAF extending inward to the black hole. The mass accretion rate in the model is essentially fixed by the X-ray data point to be of order $0.014\alpha_{-1} M_{\odot} \text{ yr}^{-1}$; Lasota et al. take $\alpha_{-1} = 1$. One free parameter remains: r_{tr} . At the time Lasota et al. (1996) was written the data did not constrain r_{tr} . Two results have since appeared that do: the 22 GHz upper limit of Herrnstein et al. (1998), and the IR detections of Chary & Becklin (1997). There has also been considerable improvement in the calculation of the ADAF model spectral energy distribution. Relativistic effects (Gammie & Popham (1998), and references therein) and advective heating of the electrons (Nakamura et al. (1997)) are now included; details of the computation are described in Narayan et al. (1998), which applies the ADAF model to the Galactic Center source Sgr A*.

Figure 3 shows the spectral energy distribution of NGC 4258 corresponding to three ADAF models, with $r_{tr} = (10, 10^{1.5}, 10^2) \times 2GM/c^2$ and $\dot{M} = (0.012, 0.008, 0.006) M_{\odot} \text{ yr}^{-1}$, which we call models 1, 1.5, and 2. The disk outside r_{tr} is thin, flat, and radiates like a blackbody. All models use the standard values for other parameters: $\alpha = 0.3, \beta = 0.5$, and $\delta = 10^{-3}$ ($\beta \equiv p_{gas}/p_{tot}$, $\delta \equiv$ fraction of dissipation going into electrons). Model 1 has the most (least) flux in the optical (radio). Evidently model 1 fits the IR data best and does not violate the 22 GHz upper limit, although the model 1.5 also gives an acceptable fit to the IR data and may have better agreement with the spectral index of the scattered optical light. Model 2 is close to violating the 22 GHz upper limit.

The ADAF model predicts the flux from the central accretion flow at several wavelengths that may be observed in the near future. At $10\mu\text{m}$ the observed flux should not be below the thin disk value (see equation [8]) of $(200, 150, 130) \cos(i)$ mJy for models (1, 1.5, 2); it can be larger because of reradiation by dust. At 22 GHz the flux should be $(0.017, 0.082, 0.23)$ mJy with $s \equiv d \ln f_{\nu} / d \ln \nu \approx 1.5$ for all three models. Higher frequency interferometry may be possible; at 100 GHz, $f_{\nu} = (0.13, 0.65, 1.5)$ mJy, with $s = (1.8, 1.4, 1.3)$, and at 690 GHz, $f_{\nu} = (3.4, 10., 18.)$ mJy, $s = (1.6, 1.3, 1.0)$. At 5500\AA the expected flux is $(38, 8.4, 0.59)$ mJy with $s = (-0.39, -2.0, -2.2)$; recall that Wilkes et al. (1995) find $s = -1.1$. The model is adjusted so that the flux at 10 keV fits the observations; at 10 keV the predicted photon index is $(1.9, 1.9, 2.0)$, which may be compared with the observed index of 1.78 ± 0.29 . Finally, the expected flux at 30 keV is $(3.1, 3.4, 3.4) \times 10^{-6} \text{ ph cm}^{-2} \text{ s}^{-1} \text{ keV}^{-1}$, and the photon index for all three models is 2.0.

4.3. Ion Torus Model

A related, though distinct, alternative to the ADAF is the ion torus (Rees et al. (1982)). As in the ADAF, it is assumed that the plasma is two-temperature with most of the pressure being supplied by the ions (see Shapiro et al 1976 for the first application of the two-temperature idea to accretion) and that the radiative losses are small. The viscosity is assumed to be small enough (low α), however, that poloidal motion can be ignored in the equation of hydrostatic equilibrium. In its simplest manifestation, the specific angular momentum is constant and the surface of the torus is a surface of constant binding energy. As the radiative losses are small, the binding energy is quite low (relative to c^2 per unit mass) and plasma flows onto the black hole through an equatorial cusp with this energy and consistent with having lost little of its binding energy. This approach can accommodate the peculiarly relativistic features of the Kerr metric (Abramowicz, Jaroszyński & Sikora (1978)).

Following previous work on thick disks, the ion torus model simply specifies the angular momentum profile rather than solving an angular momentum equation, and this is a serious weakness. Also, the model has no ready prescription for describing the gas inflow and, consequently, the thermal structure. In addition, tori of this sort are subject to hydrodynamical instability (Papaloizou & Pringle (1984)), which calls into question the assumption of slow angular momentum transport.

Nonetheless, ion tori do have one feature that is important in the present context: they naturally create a pair of funnels in which magnetic flux can be concentrated so as to extract energy from the central spinning black hole and power the jets. According to the work of Narayan, Kato & Honma (1997) and Gammie & Popham (1998), funnels are likely to be most prominent in low- α flows (ion tori), and are much less pronounced in high- α flows (standard ADAFs).

4.4. General Constraints

The failure to detect radio emission from the location of the black hole has some more general implications. Although we have demonstrated that ADAF models can be made to be consistent with this upper limit, alternative models that admit a non-thermal distribution of relativistic electrons to be accelerated directly are quite tightly constrained.

Let us suppose that there is a radio photosphere where the optical depth to synchrotron self-absorption becomes unity. Let it be located at a radial distance $r_p = 10^{14} r_{p14}$ cm from the black hole. The 22 GHz upper bound on the flux implies that

the radio brightness temperature of this photosphere must satisfy

$$T < 2 \times 10^{11} r_{p14}^{-2} \text{ K} \quad (11)$$

(Herrnstein et al. (1997a)). The corresponding energy of the electrons emitting at 22 GHz is $\sim 3kT \sim E_p \sim 70B_p^{-1/2} \text{ MeV}$. These electrons radiate at $\sim \gamma^2 B \text{ MHz}$ (cf. Rybicki & Lightman (1979)), and so we conclude that the magnetic field strength at the photosphere satisfies $B_p = B(r_p) \gtrsim r_{p14}^4 \text{ G}$, (assuming that it is significantly less than the cyclotron field, $\sim 7000 \text{ G}$). In other words the magnetic pressure must satisfy $P_{\text{mp}} \gtrsim 0.04 r_{p14}^8$, measured in dyne cm^{-2} . We use the theory of synchrotron radiation to solve for the radius of the 22 GHz photosphere:

$$r_{p14} \sim 10 f_e P_{\text{mp}}^2, \quad (12)$$

where f_e is the ratio of the emitting electrons to the magnetic pressure. Now, in order not to exceed the radio flux upper limit, we require that $r_{p14} \lesssim 1.3 f_e^{0.07} \sim 20 (GM/c^2) f_e^{0.07}$ and, equivalently, $P_{\text{mp}} \lesssim 1.1 f_e^{-0.03} \text{ dyne cm}^{-2}$. As emphasized below, however, typical pressures in accretion flows are generally expected to exceed $\sim 1 \text{ dyne cm}^{-2}$ by a large factor, so this is a fairly stringent constraint.

ADAF models satisfy this constraint because they ignore extraneous relativistic particle acceleration so that the electron distribution function is thermal and exponentially declining at energies below E_p . (Mahadevan & Quataert (1997) have shown that the thermalization time scale for the electrons in an ADAF is shorter than the flow time scale, so that the assumption of a thermal particle distribution is consistent.) What we see from the analysis in this section is that this assumption is necessary.

Disk corona models generally do postulate relativistic particle acceleration. The accelerated particles might be expected to cause observable radio emission, and so the limit on the 22 GHz brightness temperature is a serious constraint.

There are some processes which can suppress radio synchrotron emission. The Razin effect is important at densities above $\sim 10^9 B_p \text{ cm}^{-3}$. Secondly, relativistic Coulomb interactions and synchrotron loss may cool freshly accelerated electrons to keep their steady pressure at a low level. This happens on time scales competitive with the inflow timescale. Thirdly, extrinsic free-free absorption may extinguish the radio source. Two difficulties with this explanation are that the southern jet can be seen through the accreted gas at a projected perpendicular distance from the black hole of $\sim 6000 GM/c^2$ and that there is no observed soft X-ray absorption.

5. JET

It is clearly of interest to relate the observed VLBI jets to the gas flow close to the black hole. If we consider the northern VLBI component, we find that, at a projected distance of $r_{\perp} \sim 4 \times 10^{16} \text{ cm}$, the 22 GHz flux density is $\sim 3 \text{ mJy}$. If we suppose that the unresolved source is the base of a jet with an opening angle of $\sim 10^\circ$ (cf. Herrnstein et al. (1997a)) propagating nearly perpendicular to the line of sight with a bulk Lorentz factor Γ , then the radio brightness temperature is only $\sim 2 \times 10^9 \text{ K}$. Even allowing for relativistic beaming this is too low for synchrotron self-absorption to be important and it seems reasonable to assume that both radio components are optically thin at this frequency. Let us now assume that the relativistic energy density in the jet is not much smaller than the magnetic energy density. A straightforward calculation relates the minimum power carried by the relativistic electrons (and, quite possibly, positrons) in the jet to Γ and to the ratio of the electron energy density to the magnetic energy density β_e (assumed > 1):

$$L_{\text{jet}} \sim 7 \times 10^{42} \beta_e^{0.4} \left(\frac{\Gamma}{10} \right)^{3.4} \text{ erg s}^{-1} \quad (13)$$

(see, e.g., Blandford (1990)). The strong dependence of the minimum jet power upon the Lorentz factor is due to a combination of the bulk energy and the diminution of the observed flux by relativistic beaming when the observer is located roughly perpendicular to the jet direction. We see that if jets have ultrarelativistic flow speeds, then they probably carry off significantly more power than is radiated directly.

The power in the jet may be extracted directly from the spin of the black hole (Blandford & Znajek (1977)). If instead, the power is derived from the accretion flow, then the jet implies a certain minimum mass accretion rate

$$\dot{M} \sim 1.2 \times 10^{-3} \epsilon_{-1}^{-1} \beta_e^{0.4} \left(\frac{\Gamma}{10} \right)^{3.4} M_{\odot} \text{ yr}^{-1}. \quad (14)$$

Notice that this is similar to the estimates of \dot{M} obtained earlier by fitting the observed infrared spectrum.

The pressure in the jet $\sim 0.07 \beta_e^{0.4} (\Gamma/10)^{1.4} (r/4 \times 10^{16} \text{ cm})^{-2} \text{ dyne cm}^{-2}$ must be confined transversely. If we evaluate this at the transition radius of the ADAF solution, then the jet pressure is $\sim 700 (\Gamma/10)^{1.4} \beta_e^{0.4} \text{ dyne cm}^{-2}$. For comparison, the pressure in the ADAF flow is

$$P \sim 8000 \left(\frac{\dot{M}}{10^{-2} M_{\odot} \text{ yr}^{-1}} \right) \alpha_{-1}^{-1} \left(\frac{r_{\text{tr}}}{60 GM/c^2} \right)^{-5/2} \text{ dyne cm}^{-2} \quad (15)$$

We note that, although the formation of funnels appears to be problematic in ADAFs with $\alpha \gtrsim 0.01$ (Narayan, Kato & Honma (1997), Gammie & Popham (1998)), the pressure required to confine a jet able to account for the observed radio sources is probably present. An ion torus, by contrast, naturally forms a torus and can exert more pressure than a high- α ADAF as long as it is unable to cool. If the accretion rate is $\lesssim 10^{-4} M_{\odot} \text{ yr}^{-1}$, however, it does not seem possible to supply enough pressure to confine a relativistic jet.

6. DISCUSSION

We have argued that the outer, masing disk in NGC 4258 is unlikely to be in a steady state because of its long viscous timescale. Thus it is questionable whether conditions in the masing disk can be used to estimate the mass accretion rate onto the central black hole.

We have fit several models to the spectral energy distribution of the nucleus in order to better constrain the accretion rate. The ADAF model is able to fit all the data as long as $\dot{M} \approx 10^{-2} M_{\odot} \text{ yr}^{-1}$, and the transition radius (where the accretion flow makes the transition from a thin disk to an ADAF) is $\approx (10 - 100)GM/c^2$. The ADAF accretion rate is basically fixed by the X-ray luminosity, but it is nicely consistent with the observed infrared flux as long as the infrared is generated by a thin, flat disk with inclination close to that of the masing disk.

We have also fit pure thin disk models to the infrared data. (The X-ray flux would presumably be generated by a hot corona, but we have not constructed an explicit corona model, since coronae are not as tightly constrained as ADAFs.) The inferred accretion rate is strongly inclination dependent. For $i = 82^{\circ}$, $\dot{M} = 0.013 M_{\odot} \text{ yr}^{-1}$. A lower accretion rate of $0.0012 M_{\odot} \text{ yr}^{-1}$ is obtained by giving the disk an inclination of 45° , although such a low inclination seems unlikely given the orientation of the large scale jet. The accretion rate can be further lowered by giving the disk a warp that reprocesses radiation from the central source into the infrared. Since the warp parameter space is large, we have calculated the spectrum of a representative model disk with a modest warp, and the implied accretion rate is $8 \times 10^{-4} M_{\odot} \text{ yr}^{-1}$. The accretion rate might be pushed lower by a somewhat artificial positioning of reprocessing gas at the right radius; this could push the accretion rate as low as $7 \times 10^{-5} (2.1)^s \epsilon_{-1}^{-1} M_{\odot} \text{ yr}^{-1}$, where s is the slope of the intrinsic spectrum. For $s = -1$, $\epsilon_{-1} = 1$, and $\alpha_{-1} = 1$ (larger values seem unlikely except possibly in the event of gravitational instability), this minimal accretion rate is still larger than the $7 \times 10^{-6} \alpha_{-1} M_{\odot} \text{ yr}^{-1}$ obtained by Neufeld

& Maloney (1995) from consideration of the masing disk.

The minimum power in the jet in NGC 4258 also constrains the mass accretion rate, provided the jet power is derived from the accretion flow and not from the spin of the black hole. The resulting estimate for \dot{M} (cf. equation [14]) is similar to that obtained by fitting the infrared spectrum.

The limit on the 22 GHz radio flux in NGC 4258 constrains the transition radius in any ADAF to less than 100 Schwarzschild radii, as emphasized by Herrnstein et al. (1998). As we show in this paper, the flux limit also constrains corona models. If the observed X-ray emission in NGC 4258 is from a corona, then the corona must be primarily thermal rather than non-thermal, since otherwise it would produce more radio flux than observed. This limits the kinds of relativistic acceleration one can invoke in the corona.

New data at several different frequencies would give interesting information on the nature of the central accretion flow in NGC 4258. The ADAF model predicts a complete spectrum whose amplitude and slope can be compared with new data in the radio, millimeter, infrared, and X-ray; the predicted values are given in §4.

It would be particularly interesting to know if the near infrared flux is reprocessed or not. This can be tested by looking for variation on a timescale $t_r = r_{1500}/c \simeq 5.5 \times 10^5 L_{42}^{1/2} \text{ s}$, which is about a week. Since the viscous timescale—indeed, even the dynamical timescale—is much longer than this in the disk at r_{1500} , we would not expect significant variation in this component of the flux unless the infrared flux is reprocessed, or the infrared flux is produced nonthermally. If a significant fraction of the H and K band flux is reprocessed, this would rule out our simplest models and we would be forced to invoke a warped disk, wind, or other arrangement of reprocessing gas. Higher angular resolution mid-infrared data would also be interesting, since a flat disk predicts a steeper spectrum in the mid-infrared than a warped, reprocessing disk.

Finally VLBI observations at lower frequencies than 22 GHz may tighten the general constraints on relativistic particle acceleration close to the black hole and exclude free-free absorption as a factor. They may also be able to determine the onset of self-absorption in the jet and thence provide a stronger constraint on the pressure and jet power by allowing us to solve for the magnetic field strength. Further monitoring of the variability in both the northern and the southern component may also help determine the jet speed and elucidate the relationship between the jets and gas flow within ~ 100 gravitational radii of

the central black hole.

This work was supported in part by NSF grants

AST 94-23209, AST 95-29170, and NASA grants NAG 5-2837, NAG5-7007. We thank A. Esin for assistance with the ASCA data.

REFERENCES

- Abramowicz, M. Jaroszyński, M. & Sikora, M. 1978, *A&A*, 63, 221
- Abramowicz, M., et al. 1995, *ApJ*, 438, L37.
- van Albada, G.D., & van der Hulst, J. M. 1982, *A&A*, 115, 263
- Blandford, R.D. 1990, in *Active Galactic Nuclei*, Saas-Fee Advanced Course 20. (Berling: Springer-Verlag).
- Blandford, R. D. 1998 *Proc. Maryland Conference on Astrophysics*. "Some Like it Hot". ed. S. Holt & T. Kallman, New York: AIP
- Blandford, R.D., & Znajek, R. L. 1977, *MNRAS*, 179, 433.
- Cao, X., & Jiang, D.R. 1997, *A&A*, 322, 49
- Cardelli, J.A., Clayton, G.C., & Mathis, J.S. 1989, *ApJ*, 345, 245
- Cecil, G., Wilson, A.S., & DePree, C. 1995, *ApJ*440, 181
- Cecil, G., Wilson, A.S., & Tully, R.B., 1992, *ApJ*, 390, 365
- Cecil, G., Morse, J.A., & Veilleux, S. 1995, *ApJ*, 452, 613
- Chary, R., & Becklin, E. E. 1997, *ApJ Lett*, 485, L75
- Chiang, E.I., & Goldreich, P. 1997, *ApJ*, 490, 368
- Cizdziel, P.J., Wynn-Williams, C.G., & Becklin, E.E. 1985, *AJ*, 90, 731
- Claussen, M.J., Heiligman, G.M., & Lo, K.Y., *Nature*, 310, 298
- Claussen, M.J., & Lo, K.Y., *ApJ*308, 592
- Courtès, G., & Cruvellier, P. 1961, *CR Acad. Sci. Paris*, 253, 218
- Gammie, C.F., & Popham, R. 1998, *ApJ*, 498, 313.
- Greenhill, L.J. et al., 1994, in "Highlights of Astronomy, Vol. 10" (Dordrecht: Kluwer) p. 531
- Greenhill, L.J. et al., 1995, *ApJ*, 440, 619
- Greenhill, L.J. et al., 1995, *A&A*, 304, 21
- Haardt, F., & Maraschi, L. 1991, *ApJ*, 380, 51
- Haschick, A.D., & Baan, W.A. 1990, *ApJ*, 355, L23
- Haschick, A.D., Baan, W.A., & Peng, E.W. 1994, *ApJ*, 356, 149
- Herrnstein, J.R. 1997, PhD thesis, Harvard University
- Herrnstein, J.R. et al. 1998, *ApJ*, 497, 69
- Herrnstein, J.R., Greenhill, L., & Moran, J. 1996, *ApJ*, 468, L17
- Herrnstein, J.R., et al., 1997, *ApJ Lett*, 475, L17
- Herrnstein, J.R., et al. 1997, abstract published in *BAAS*, 191, #25.07
- Ichimaru, S. 1977 *ApJ*, 214, 840.
- Konigl, A., & Kartje, J.F., 1994, *ApJ*, 434, 446
- van der Kruit, P. C., Oort, J.H., & Mathewson, D. S. 1972, *A&A*, 21, 169
- Kumar, P. 1997, *ApJ*, submitted (astro-ph 9706063)
- Laor, A., & Draine, B.T., 1993, *ApJ*, 402, 441
- Lasota, J.P., et al. 1996, *ApJ*, 462, 142
- Mahadevan, R., & Quataert, E. 1997, *ApJ*, 490, 605
- Makishima, K., et al., 1994, *PASJ*, 46, L77
- Maoz, E., & McKee, C. F. 1997, *ApJ*, submitted (astro-ph 9704050)
- Martin, P., Roy, J.-R., Noreau, L., & Lo, K.Y. 1989, *ApJ*, 345, 707
- Miyoshi, M., et al. 1995, *Nature*, 373, 127
- Moran, J.M., et al. 1995, *PNAS*, 92, 11427
- Nakai, N., Inoue, M., & Miyoshi, M., 1993, *Nature*, 361, 45
- Nakamura, K.E. et al. 1997, *PASJ*, 49, 503.
- Narayan, R. 1997, in *Proceedings of IAU Colloquium 163, Accretion Phenomena and Related Objects*, A. S. P. Conference Series, eds. D. T. Wickramasinghe, L. Ferrario, & G. V. Bicknell, p.75
- Narayan, R., & Yi, I. 1994, *ApJ*, 428, 13.
- Narayan, R., Kato, S. & Honma, F., 1997, *ApJ*, 476, 49
- Narayan, R., & Yi, I. 1995, *ApJ*, 444, 231.
- Narayan, R., & Yi, I. 1995, *Nature*, 374, 623.
- Narayan, R., et al. 1998, *ApJ*, 492, 554
- Narayan, R., Mahadevan, R., & Quataert, E. 1998, to appear in "The Theory of Black Hole Accretion Discs", eds. M.A.Abramowicz, G.Bjornsson, & J.E.Pringle (Cambridge) (astro-ph 9803141)
- Neufeld, D.A., & Maloney, P.R., 1995, *ApJ Lett*, 447, L17
- Papaloizou, J. C. B. & Pringle, J. E., 1984, *MNRAS*, 208, 721
- Phinney, E. S. 1989, in *Theory of Accretion Disks*, eds. W. Duschl et al. (Dordrecht: Kluwer), p. 457
- Popham, R., & Gammie, C.F. 1998, *ApJ*, in press (astro-ph 9802321).
- Pringle, J. 1981, *ARA&A*, 19, 137
- Rees, M. J., Begelman, M. C., Blandford, R. D. & Phinney, E. S. 1982, *Nature* 295 17
- Rieke, G. H., & Lebofsky, M.J., 1978, *ApJ*, 220, L37
- Rybicki, G. B., & Lightman, A. P., *Radiative Processes in Astrophysics* (New York: Wiley).
- Sanders, D.B., et al. 1989, *ApJ*, 347, 29
- Shakura, N.I., & Sunyaev, R. A. 1973, *A&A*, 24, 337
- Shapiro, S. L., Lightman, A. P. & Eardley, D. M. 1976 *ApJ*, 204, 187
- Spitzer, L., 1978, *Physical Processes in the Interstellar Medium* (New York: Wiley)
- Watson, W.D., & Wallin, B.K., 1994, *ApJ Lett*, 432, L35
- Wilkes, B.J., et al. 1995, *ApJ*, 455, L13

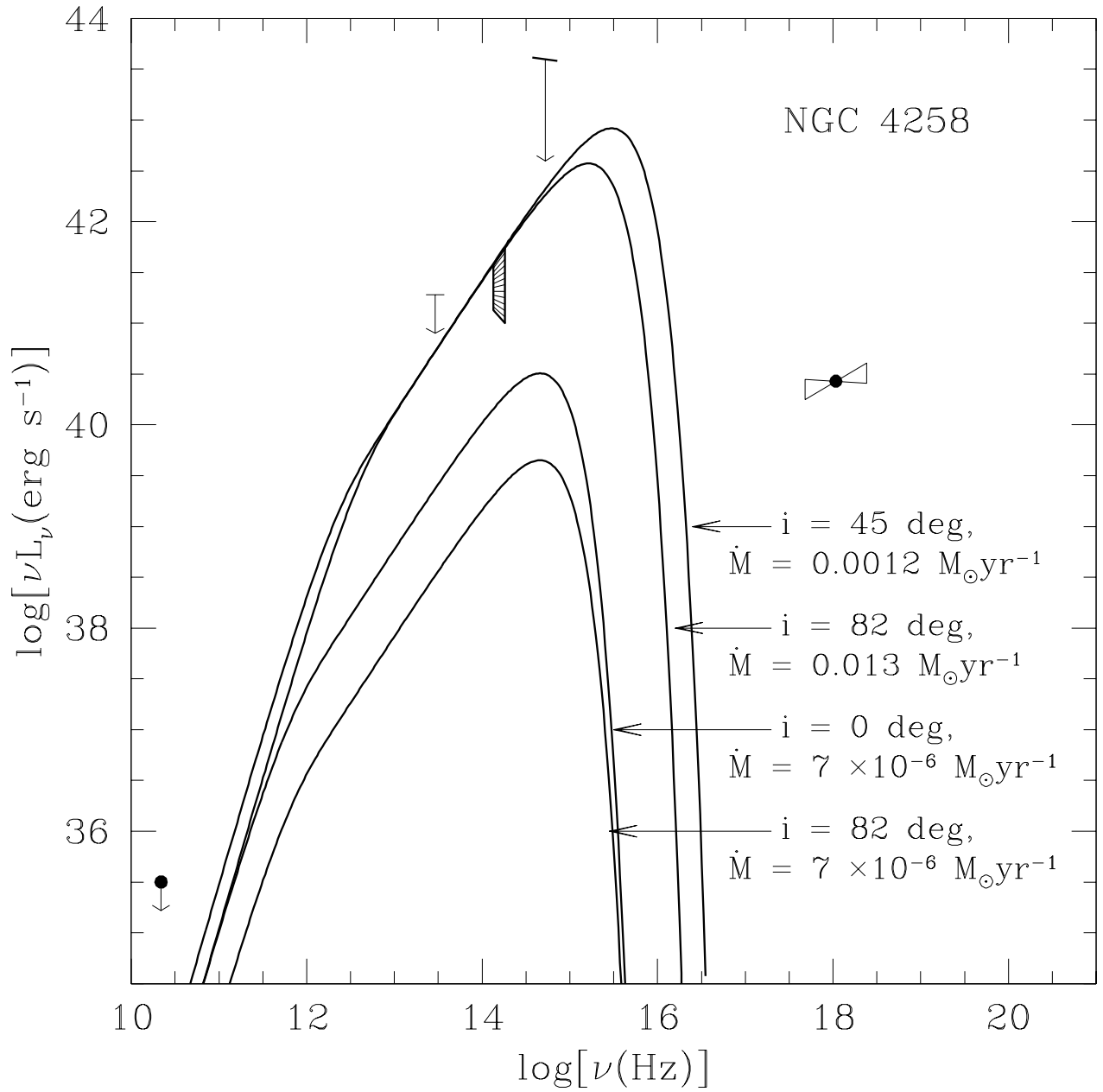


FIG. 1.— The spectral energy distribution of the nucleus of NGC 4258. The data points are described in the text (see §2). The models are flat, thin disks with inclination $i = (45, 82, 0)^\circ$ and $\dot{M} = (0.0012, 0.013, 7 \times 10^{-6}) M_\odot \text{yr}^{-1}$.

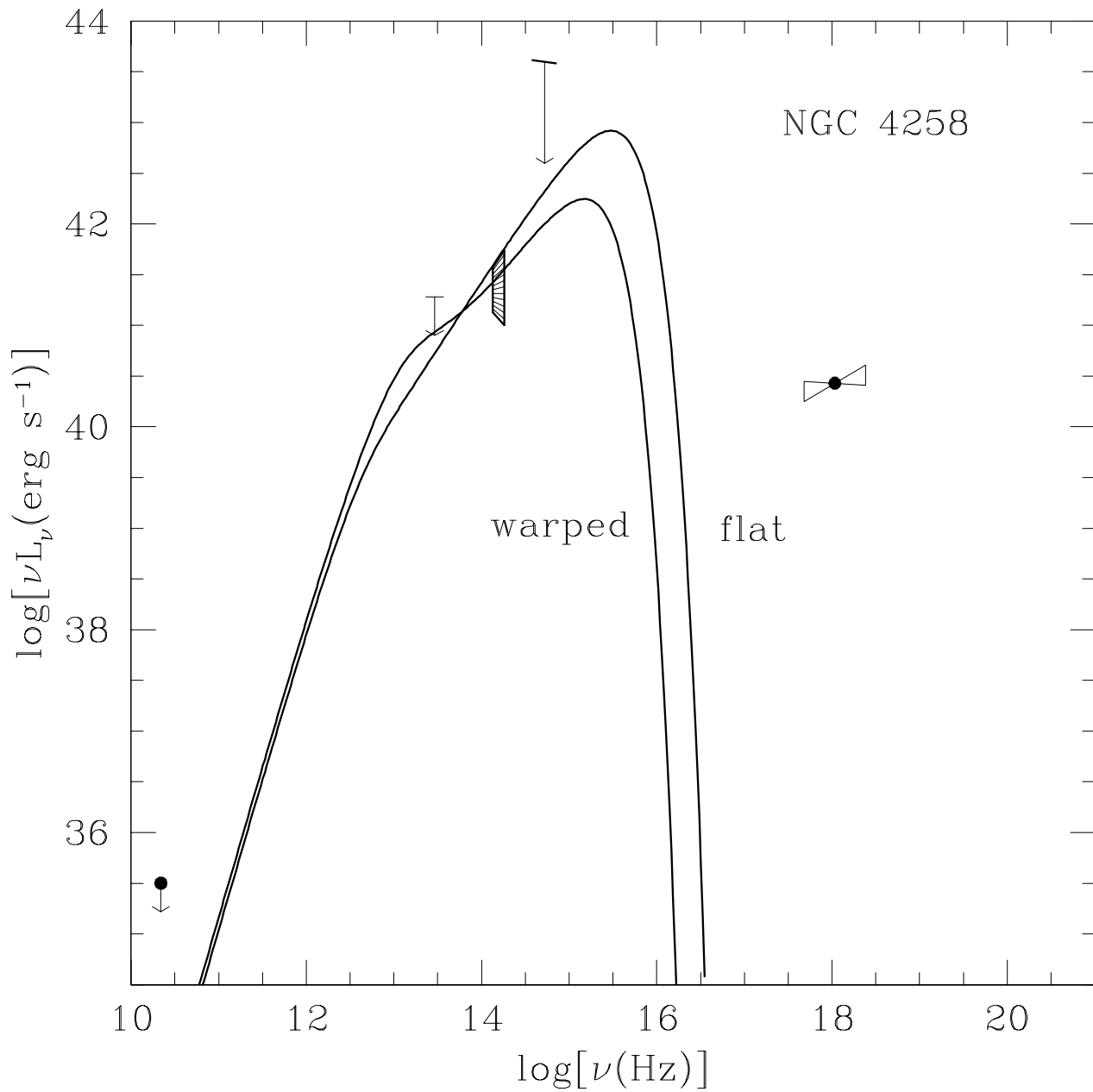


FIG. 2.— Same as Figure 1, but for a warped, reprocessing disk with $\dot{M} = 0.0008 M_\odot \text{ yr}^{-1}$ as well as the flat disk model with $i = 82^\circ$ and $\dot{M} = 0.013 M_\odot \text{ yr}^{-1}$.

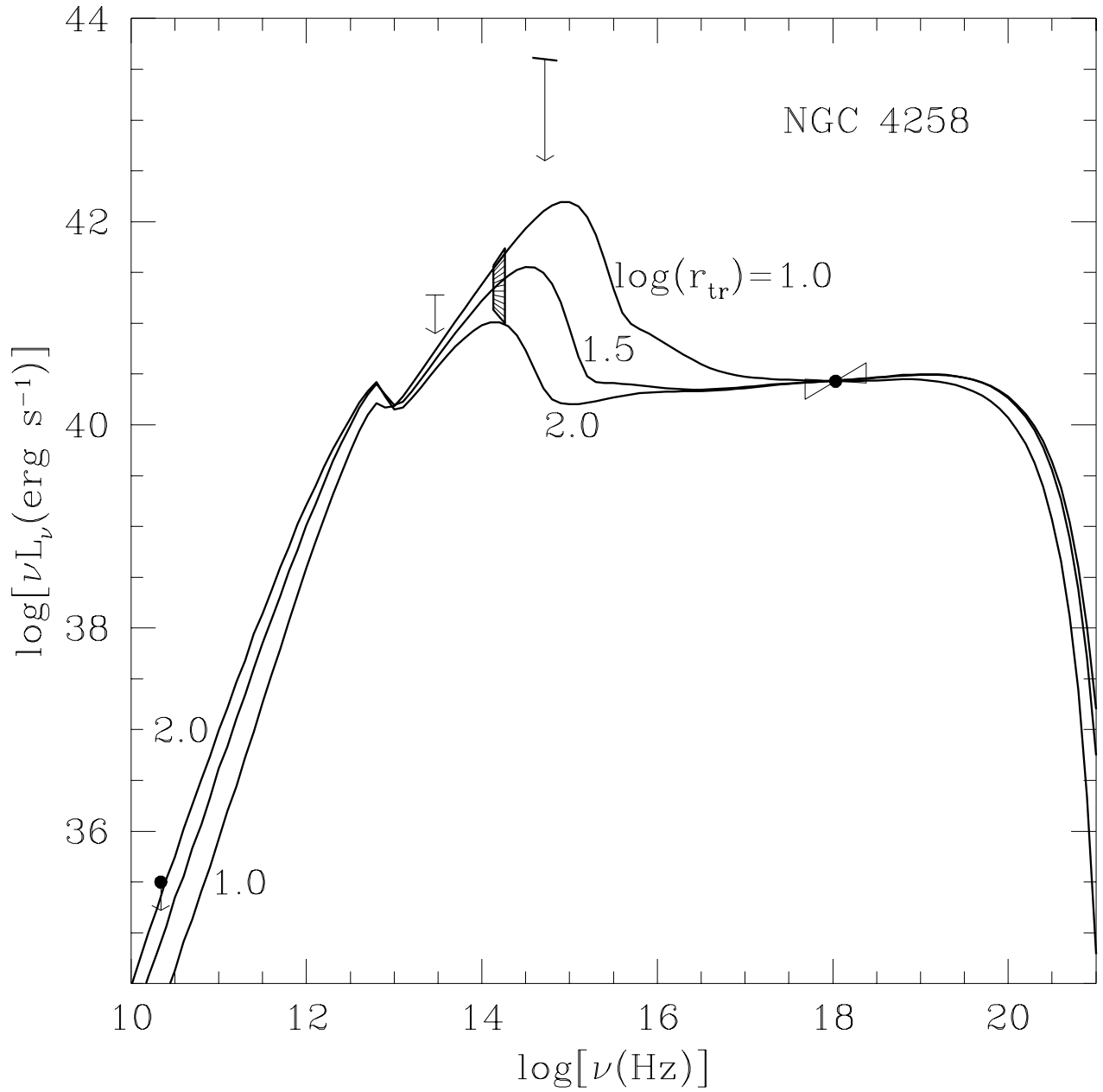


FIG. 3.— The models are ADAFs fit with $r_{\text{tr}} = (10, 10^{1.5}, 10^2)2GM/c^2$ and $\dot{M} = (0.012, 0.008, 0.006) M_\odot \text{yr}^{-1}$. As the transition radius moves in the optical/IR flux increases.